Catalysis Today 183 (2012) 34–41

Contents lists available at SciVerse ScienceDirect

Catalysis Today

journal homepage: www.elsevier.com/locate/cattod

Alkyl sulfonated diphosphines-stabilized ruthenium nanoparticles as efficient nanocatalysts in hydrogenation reactions in biphasic media

M. Guerrero[a,b], A. Roucoux[c,d], A. Denicourt-Nowicki[c,d], H. Bricout[e], E. Monflier[e], V. Collière[a,b], K. Fajerwerg[a,b], K. Philippot[a,b,*]

[a] CNRS; LCC (Laboratoire de Chimie de Coordination); 205, Route de Narbonne, F-31077 Toulouse, France
[b] Université de Toulouse; UPS, INPT; LCC; F-31077 Toulouse, France
[c] Ecole Normale Supérieure de Chimie de Rennes, CNRS, UMR6226, Avenue du Général Leclerc, CS 50837, F-35708 Rennes Cedex 7, France
[d] Université européenne de Bretagne, France
[e] UMR CNRS 8181; Université d'Artois, Faculté des Sciences Jean Perrin, Rue Jean Souvraz, SP 18, F-62307 Lens Cedex, France

ARTICLE INFO

Article history:
Received 28 July 2011
Received in revised form 8 September 2011
Accepted 11 September 2011
Available online 4 October 2011

Keywords:
Sulfonated diphosphine
Ruthenium
Nanoparticles
Biphasic catalysis
Hydrogenation
Water

ABSTRACT

The organometallic synthesis of ruthenium nanoparticles stabilized by water-soluble alkyl sulfonated diphosphines as ligands is described for the first time. After isolation, the so-obtained nanoparticles could be easily dispersed into water giving rise to stable aqueous colloidal solutions without precipitation over the course of several months. The catalytic behaviour of these aqueous colloidal solutions has been investigated in the hydrogenation of unsaturated substrates (tetradecene, styrene and acetophenone) in biphasic liquid–liquid conditions, showing interesting results in terms of reactivity. Interestingly, small structural differences in the backbone of the diphosphine ligands influence the catalytic activity of these nanocatalysts. In addition, preliminary tests of recycling showed promising results with neither loss of activity or significant precipitation.

1. Introduction

The synthesis of well-controlled nanometric size metal species has received a considerable attention over the past decades due to their attractive physical and chemical properties that lead to numerous applications in various fields [1]. Among them, catalysis is a tremendous active research domain where metal nanoparticles are extensively used by the international scientific community [2]. This interest mainly follows from the fact that metal nanoparticles provide an efficient combination of heterogeneous and homogeneous catalysts advantages such as a high specific surface area resulting in a high number of potential catalytic sites as well as the possibility to tune their surface properties. In the particular case of colloidal catalysis where metal nanoparticles are dispersed in a solvent, the development of nanocatalysts active in various reaction conditions such as in organic solvents, water, ionic liquids or even supercritical fluids depending on the target reactions is of high importance. Indeed, as the separation of expensive transition metal catalysts from substrates and products is a key-point for industrial applications, it is necessary to develop simple methods for the preparation of appropriate metal nanocatalysts according to the reaction conditions [3].

Besides the C–C coupling reactions, metal nanoparticles are also widely investigated in hydrogenation reactions [4]. Water-soluble metal nanocatalysts are commonly used in the hydrogenation of monocyclic arenes under mild conditions [5] and continue to attract attention as potential “green” approaches due to increased economic and environmental concerns [6]. Nevertheless, the development of modified nanoparticles for total or partial arene hydrogenations is still a challenging issue and remains an active area of research since these reactions represent an important chemical process for the synthesis of fine chemicals [7]. These later are widely used for various applications from laboratory to industrial scale process such as, for example, the obtaining of cyclohexane for the production of nylon-6,6 [8]. Another interesting aspect lies in the fact that the activity and the selectivity of nanocatalysts can be tuned by the choice of suitable ligands for their stabilization, as ligands can modulate the environment of the metal surface through electronic/steric modifications. In the same way, ligands can be used to adapt metal nanoparticles to chosen reaction conditions as they can transfer them their own solubility properties [9].

---

* Corresponding author at: CNRS; LCC (Laboratoire de Chimie de Coordination); 205, Route de Narbonne, F-31077 Toulouse, France. Tel.: +33 561333230; fax: +33 561553003.
E-mail address: karine.philippot@lcc-toulouse.fr (K. Philippot).

0920-5861/$ – see front matter © 2011 Elsevier B.V. All rights reserved.
doi:10.1016/j.cattod.2011.09.012

As previously done for homogeneous catalysts, biphasic liquid–liquid systems represent an attractive alternative for recovering aqueous soluble catalysts after separation from the organic phase containing products [10]. For that purpose, complexes containing water-soluble phosphines as ligands [11] constitute an interesting example of catalysts that are retained in the aqueous phase, the most widespread ligand being the sodium salt of trisulfonated triphenylphosphine, which is industrially applied in the hydroformylation of propene and butene [12] as well as in the Suzuki coupling of non activated aryl bromides [13].

In that context, and on the base of our previous works with phosphine derivatives [14] and 1,3,5-triaza-7-phosphaadamantane (PTA) [15] as stabilizing ligands for the synthesis of metal nanoparticles, we explored the use of alkyl sulfonated diphosphines as water-soluble ligands to obtain ruthenium nanoparticles in aqueous phase. These latter are suitable nanocatalysts for their further use in biphasic liquid–liquid hydrogenation reactions, the organic phase being the substrate. To the best of our knowledge, there are only a few examples using sulfonated phosphines as ligands for metal nanoparticles stabilization [16]. In this work we report the first one concerning ruthenium nanoparticles.

These Ru(0)NPs have been characterized by elemental analysis, low and high resolution transmission electron microscopy (TEM, HRTEM, EDX) and dynamic light scattering (DLS). As a function of the backbone of the alkyl sulfonated diphosphine ligands and thermodynamic parameters, the hydrogenation reactions of unsaturated compounds such as styrene, tetradecene and acetophenone in biphasic liquid–liquid conditions have been investigated.

2. Materials and methods

2.1. Reagents and general procedures

All operations concerning nanoparticles syntheses were carried out in Schlenck or Fischer–Porter glassware using vacuum-argon lines techniques or in a glove-box under argon atmosphere. The organometallic complex used as precursor, (1,5-cyclooctadiene)(1,3,5-cyclooctatriene)ruthenium (0) complex ([Ru(COD)(COT)]) was purchased from Nanomeps-Toulouse. Sulfonated diphosphines (1,4-bis [(di-m-sulfonatophenyl) phosphino]butane (**L1**), 1,4-bis [(di-m-sulfonatophenyl)phosphino]propane (**L2**), and 1,4-bis [(di-m-sulfonatophenyl)phosphino]ethane (**L3**)) used as stabilizing ligands were synthesized following a published procedure [17].

Solvents were dried and distilled before use: tetrahydrofurane (THF) over sodium-benzophenone and pentane over calcium hydride. All reagents and solvents were degassed before use by means of three freeze–pump–thaw cycles. Water was distilled twice by conventional method before use to prepare nanoparticles suspensions. Tetradedecene, styrene and acetophenone used as substrates in catalysis were purchased from Acros Organics or Sigma–Alfa Aesar and used without further purification.

2.2. Characterization techniques

Samples for TEM/HRTEM analyses were prepared by slow evaporation of a drop of crude colloidal solution deposited onto holey carbon-covered copper grids under argon (in glove-box) for THF solutions and under air for aqueous solutions. Transmission Electron Microscopy at low (TEM) and high resolution (HRTEM) analyses were performed at the "Service Commun de Microscopie Electronique de l'Université Paul Sabatier" (UPS-TEMSCAN). TEM images were obtained using a JEOL 1011 electron microscope operating at 100 kV with resolution point of 4.5 Å. HRTEM observations were carried out with a JEOL JEM 2010 electron microscope working at 200 kV with a resolution point of 2.5 Å and equipped with X-ray analysis PGT (light elements detection, resolution 135 eV). The size distributions were determined through a manual analysis of enlarged micrographs with Imagetool software to obtain a statistical size distribution and a mean diameter. FFT treatments have been carried out with Digital Micrograph Version 1.80.70.

2.3. Synthesis of alkyl sulfonated diphosphine-stabilized ruthenium nanoparticles

In a typical reaction, 150 mg of [Ru(COD)(COT)] (0.476 mmol) were introduced in a Fischer–Porter bottle and left in vacuum during 0.5 h and cooled to 193 K. 150 mL of THF, containing 41 mg of **L1** (0.048 mmol, [L1]/[Ru] = 0.1) were then added. The Fischer Porter bottle was heated to 298 K and then pressurized with 3 bars of dihydrogen. After 18 h, a homogenous brown colloidal solution is obtained. The volume of the solution was reduced to approximately 10 mL by solvent evaporation before its transfer onto a solution of deoxygenated pentane (100 mL). A brown precipitate formed which was filtered and dried in vacuum, giving rise to the nanoparticles as a dark brown powder. The molar of [L]/[Ru] was varied from 0.1 to 0.5 taking account previous results with diphenylphosphinobutane [14b]. In all cases, these ruthenium colloids were found to be stable with time under argon atmosphere without precipitation after a few weeks. Elemental Analysis results for the different Ru(0)NPs prepared with the molar ratio [L]/[Ru] = 0.1 are: L1 (39.1 wt% Ru); L2 (38.9 wt% Ru) L3 (38.6 wt% Ru).

2.4. Quantification of hydrides at the surface of ruthenium nanoparticles

The quantification of hydrogen atoms adsorbed onto the surface of Ru nanoparticles by GC analyses was carried out on aqueous colloidal solutions following a previously described procedure [14b]. On each fresh colloidal solution, 5 equivalents of olefin (2-norbornene), previously filtered through alumina, were added. Samples were taken from the solutions for GC analysis and estimation of the norbornene conversion into norbornane. The measurement of the amount of alkane formed by GC analysis allows to determine the necessary quantity of hydrogen atoms for reducing the alkene, and further to calculate the H/Ru_s ratio considering the nanoparticles mean sizes.

For that study, gas chromatography was performed using a HP 5890 Series II Gas Chromatograph with a SGE BP1 non polar 100% dimethyl polysiloxane capillary column of 50 m × 0.32 mm × 0.25 μm. The method used consists of 15 min. at 40 °C and a ramp of 8 °C min^{-1} until 250 °C. Conversions were determined as following: the peak area of the norbornane divided by the sum of the peak area of norbornene and norbornane.

2.5. Catalytic hydrogenation reactions

For styrene and tetradecene hydrogenation reactions gas chromatography analyses were performed using a Carlo Erba GC 6000 with an FID detector equipped with a Factor Four column (30 m, 0.25 mm i.d.). Parameters were as follows: initial temperature, 40 °C; initial time, 10 min; ramp, 10 °C min^{-1}; final temperature, 80 °C; final time, 30 min; injector temperature, 220 °C; detector temperature, 250 °C. For acetophenone hydrogenation reactions analysis a Trace GC Ultra (ThermoFisher) with a FID detector equipped with a TR5 column (30 m, 0.25 mm i.d.). Selectivities are stated as following: the peak area of the selected product (styrene, ethylbenzene, ethylcyclohexane, tetradecane, phenylethan-1-ol, cyclohexylethan-1-ol) divided by the sum of the peak area of all the products formed.

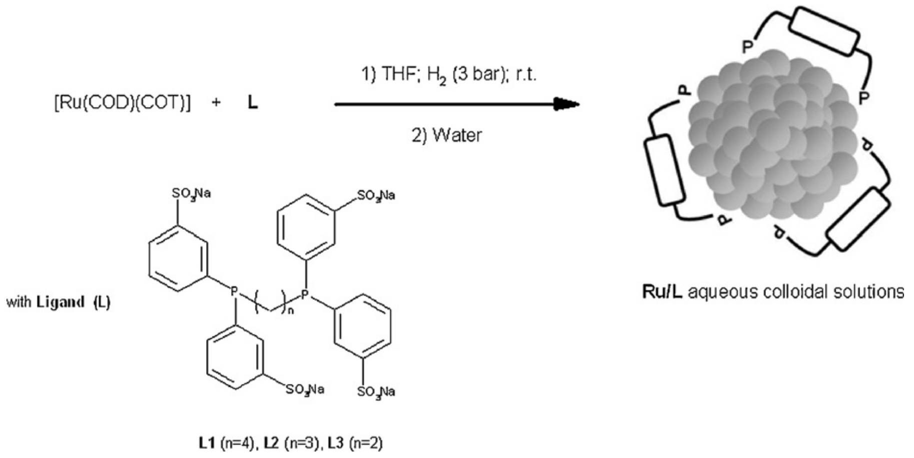

Scheme 1. Synthesis of alkyl sulfonated diphosphine-stabilized Ru(0)NPs.

2.5.1. *Atmospheric hydrogenation reactions*

A 25 mL round bottom flask, charged with 10 mL of the water colloidal suspension of Ru(0)NPs stabilized with sulfonated diphosphines **L1**, **L2** or **L3** and the appropriate amount of the organic substrate (styrene, tetradecene, acetophenone; 0.45, 1 and 0.45 mL, respectively) providing a molar ratio [Substrate]/[Metal] = 100, was connected to a gas burette (500 mL) and a flask to balance pressure. Then, the system was filled with hydrogen (P_{H2} = 1 bar) and the mixture was magnetically stirred at 1500 rpm. Samples were removed from time to time (1 h, 20 h and 40 h) to monitor the reaction by gas chromatography in previously mentioned conditions.

2.5.2. *High pressure hydrogenation reactions*

The stainless steel autoclave was charged with the aqueous suspension of the sulfonated diphosphine-stabilized Ru(0) nanoparticles and a magnetic stirrer. The investigated substrate was added into the autoclave and dihydrogen was admitted to the system at constant pressure (up to 10 bar). Samples were removed from time to time (1 h, 20 h and 40 h) to monitor the reaction by gas chromatography in previously mentioned conditions.

3. Results and discussion

3.1. *Synthesis and characterization of alkyl sulfonated diphosphine-stabilized ruthenium nanoparticles*

The ruthenium nanoparticles (RuNPs) were prepared by hydrogenation of the organometallic precursor [Ru(COD)(COT)] (COD = 1,5-cyclooctadiene; COT = 1,3,5-cyclooctatriene) in THF at room temperature (Scheme 1) in the presence of alkyl sulfonated diphosphine ligands (1,4-bis [(di-m-sulfonatophenyl) phosphino]butane (**L1**), 1,4-bis [(di-m-sulfonatophenyl)phosphino]propane (**L2**) and 1,4-bis [(di-m-sulfonatophenyl)phosphino]ethane (**L3**)) in different [ligand]/[metal] molar ratio (0.1, 0.2 or 0.5) following a previously described procedure [18]. The choice of the [ligand]/[metal] molar ratios was made on the basis of previous results obtained with alkyl diphosphines [14b].

All the Ru(0)NPs obtained in this way were found to be stable for at least three weeks in THF, demonstrating the efficiency of the three alkyl sulfonated diphosphines in stabilizing the Ru(0) nanoclusters. Analysis of the THF colloidal solutions by transmission electron microscopy (TEM) revealed the presence of small particles (Fig. 1) with a mean size in the range 1.2–1.5 nm (Table 1), which are well-dispersed on the grid.

Table 1
Mean diameters of the RuNPs according to the ligand and the [**L**]/[Ru] molar ratio.

RuNPs systems	[L]/[Ru] molar ratio	Mean size in THF, nm (SD)	Mean size in H_2O, nm (SD)
Ru/**L1**	0.1	1.51 (0.18)	1.50 (0.20)
	0.2	1.27 (0.15)	1.29 (0.18)
	0.5	1.25 (0.16)	1.26 (0.21)
Ru/**L2**	0.1	1.48 (0.19)	1.50 (0.21)
	0.2	1.26 (0.14)	1.24 (0.20)
	0.5	1.23 (0.17)	1.23 (0.24)
Ru/**L3**	0.1	1.50 (0.19)	1.52 (0.23)
	0.2	1.23 (0.16)	1.24 (0.22)
	0.5	1.23 (0.14)	1.27 (0.21)

Whatever the alkyl diphosphine used, the mean size of the particles tends to slightly decrease with the increase of the [L]/[metal] molar ratio from 0.1 to 0.2 but does not change in the presence of more ligand ([L]/[Ru] = 0.5). In addition, no significant difference in the mean sizes of the particles depending on the ligand used for their stabilization was observed although small changes are present in their backbones. In consequence, the key-parameter for the control of the mean size of the particles seems to be more related to the [L]/[metal] molar ratio than the alkyl chain between the two phosphorus atoms (see L, Scheme 1).

Afterwards, the nanoparticles were isolated as a black solid from the THF solution by precipitation with pentane addition, dried under vacuum, and easily redispersed into water leading to stable aqueous colloidal solutions for at least up to three months. The transfer into water did not induce any relevant change in dispersion and in their mean diameters as confirmed by TEM analysis (Fig. 2, Table 1).

High-resolution transmission electron microscopy (HRTEM) analysis performed from colloidal solutions in water revealed that the Ru nanoparticles are well-crystallized. They are single crystals with reticular planes extending over the entire particle as presented in Fig. 3 for the Ru/**L1** system with a mean size of 1.5 nm as previously determined by TEM. The obtained images show some nanoparticles which are well-oriented and appear crystalline (Fig. 3) and for which we could measure through Fast Fourier Transform (FFT) the lattice parameters. The measured lattice parameters appear very close to the theoretical ones expected for the hcp structure of ruthenium bulk. Moreover, Energy-dispersive X-ray spectroscopy (EDX) analysis shows a characteristic pattern of metallic ruthenium.

In order to study the mean size of the Ru nanoparticles directly in solution, dynamic light scattering experiments (DLS) of aqueous

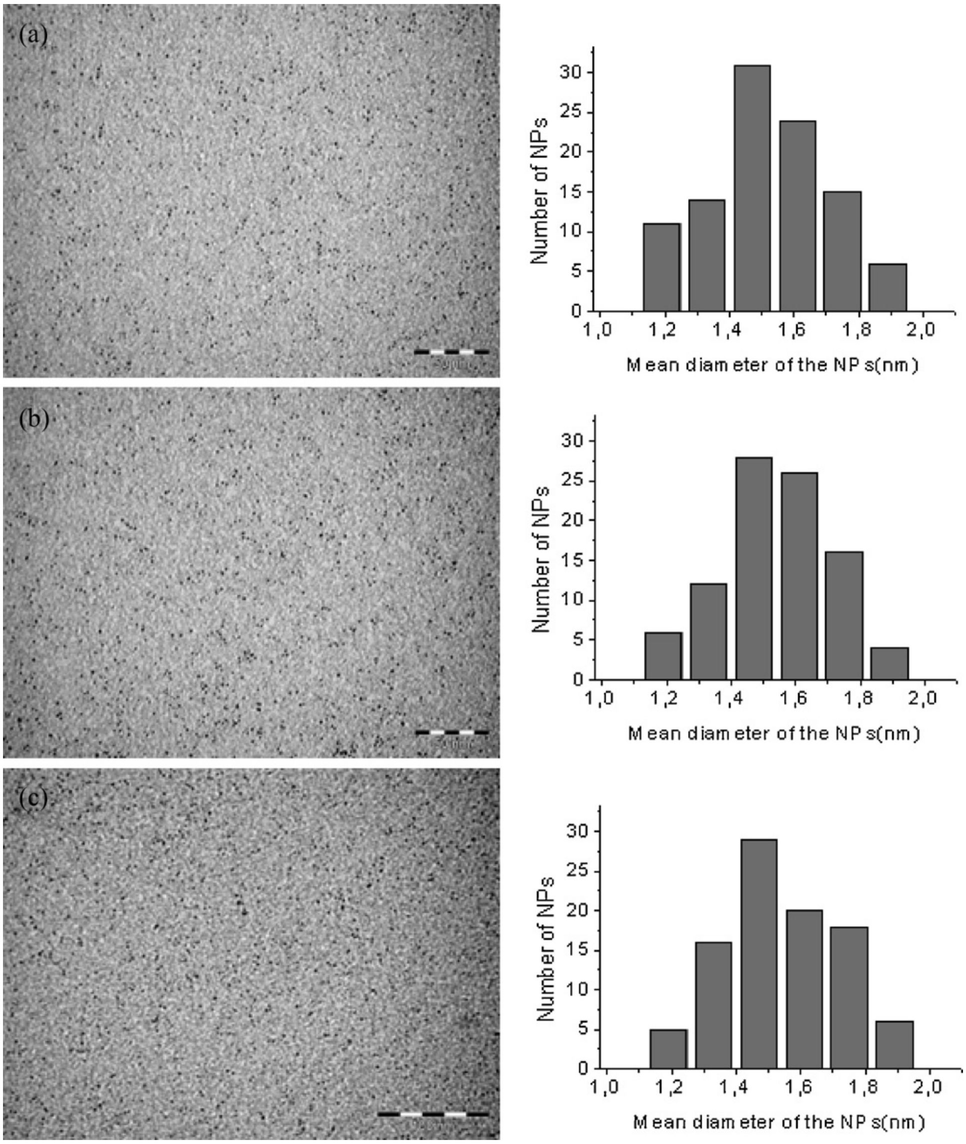

Fig. 1. TEM images of Ru(0)NPs stabilized with **L1** (a), **L2** (b) and **L3** (c) in the [**L**]/[Ru] ratio of 0.1 from THF colloidal solutions.

colloidal solutions have been performed [19]. DLS experiments are used for the accurate and fast size measurement of hydrodynamic diameter and aggregation effects of nanoparticles samples. These are important parameters for the latter application of the NPs in liquid phase catalysis. The hydrodynamic diameter takes into consideration the metallic core but also the shell of ligand present around the nanoparticles. It is thus a good method to know if the ligand is present at the surface of the particles and if they are agglomerated or not in solution. The obtained results show a good correlation between the values obtained by TEM (after evaporation of a drop of the colloidal solution on the grid) and DLS (directly in solution) as presented in Fig. 4 for the Ru/**L1** system. These results indicate that the nanoparticles are isolated and do not agglomerate in solution. In addition, they show that the ligand is present under the form of a shell surrounding the metallic core. The presented system displays a mean size of 1.8 nm by DLS against 1.5 nm by TEM (see Table 1), which allows us to estimate the ligand shell thickness to ca. 0.15 nm.

As ruthenium nanoparticles are prepared under dihydrogen atmosphere the presence of hydrides at their surface can be expected. This was confirmed by the hydrogenation model reaction of norbornene. This reaction allows the titration of surface hydrides because no extra hydrogen is added to the reaction mixture [14b]. The measurement of the amount of alkane formed by GC analysis allows to determine the necessary quantity of hydrogen atoms for reducing the alkene, and further to calculate the H/Ru_s ratio considering the nanoparticles mean sizes. This methodology was applied for aqueous colloidal solutions and revealed 1.6, 1.1, and 1.0 hydrogen atom per surface ruthenium atom for the Ru/**L1**, Ru/**L2**, and Ru/**L3** nanoparticles, respectively. These values indicate that the nanoparticles are able to activate dihydrogen. They also show a trend $L1 > L2 \approx L3$ and a significant difference for the Ru/**L1** nanoparticles system which have more hydrides at their surface. It appears thus that a longer alkyl chain is more favorable for the presence of a higher quantity of hydrides at the Ru(0)NPs surface.

In summary of this chapter, various alkyl sulfonated diphosphine-stabilized Ru(0) NPs were reproducibly prepared. Their characterization indicates small sizes, well-crystallized nanoclusters as well as the presence of hydrides at their surface. More importantly, it is obvious that the alkyl sulfonated diphosphine ligands allow their easy dissolution into water giving rise to stable aqueous colloidal solutions at least up to several months. For these

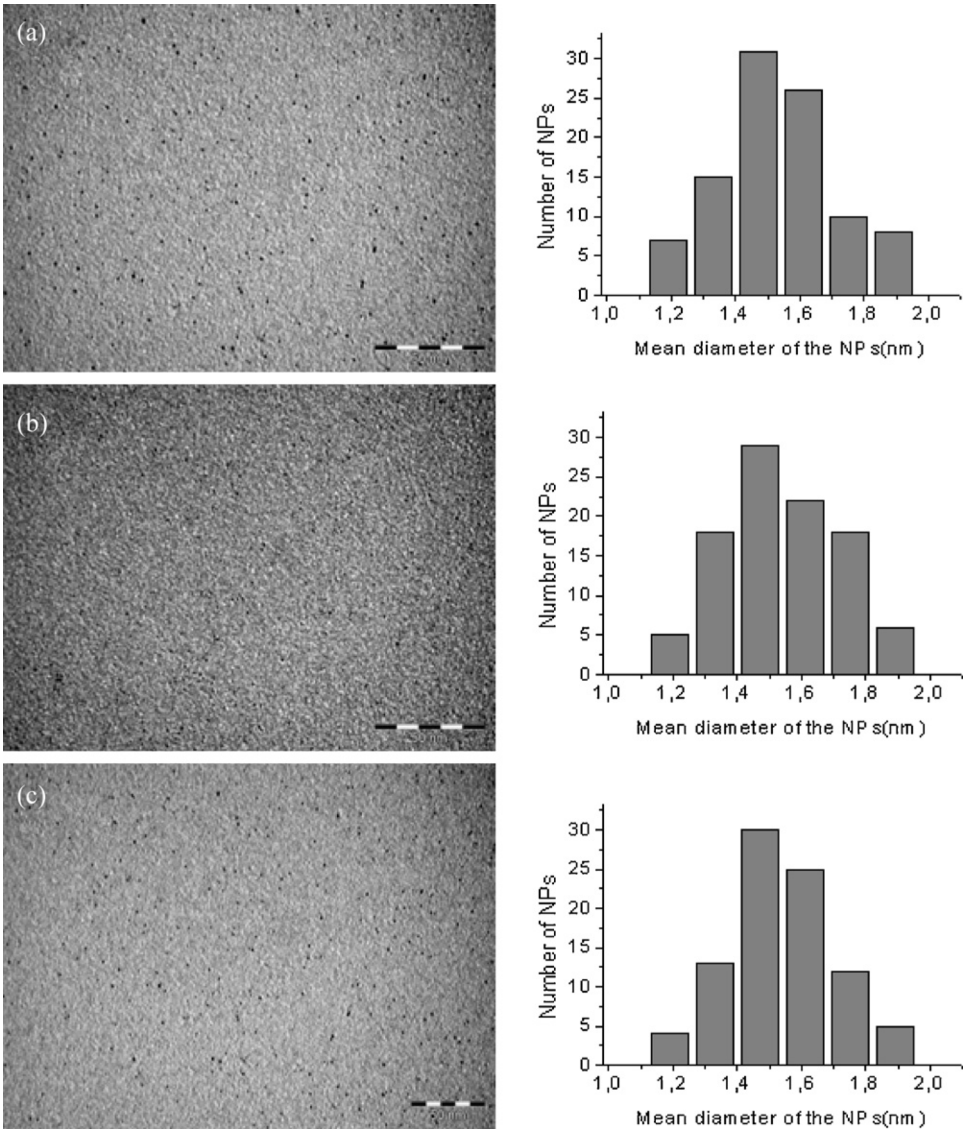

Fig. 2. TEM images of Ru(0)NPs stabilized with **L1** (a), **L2** (b) and **L3** (c) in the [**L**]/[Ru] molar ratio of 0.1 from aqueous colloidal solutions.

reasons, these new ruthenium nanoparticles provide potential nanocatalysts for hydrogenation reactions. That is why they were further investigated in hydrogenation of unsaturated substrates in biphasic liquid–liquid conditions.

3.2. Catalytic hydrogenation reactions

3.2.1. Styrene hydrogenation under atmospheric hydrogen pressure

In a first approach, performances of **L1**, **L2** and **L3** sulfonated diphosphine-stabilized Ru(0) nanoparticles used as nanocatalysts were evaluated in the hydrogenation of styrene as a pertinent model substrate due to an easily reducible exo C=C double bond and an aromatic ring. Table 2 reports the catalytic data obtained at 20 °C under H_2 at atmospheric pressure (molar ratio [L]/[Ru] of 0.1). The influence of the alkyl chain length of the ligand in the different Ru(0)NPs used as nanocatalysts on the conversion of styrene (ST) and the selectivity in ethylbenzene (EB)/ethylcyclohexane (EC) was studied. The selectivity of the reaction was evaluated according to the EB vs. EC ratios. It is noteworthy that at the chosen molar ratio [L]/[Ru] of 0.1, all Ru(0)NPs have a mean diameter of 1.5 nm in water (Table 1).

Whatever the ligand **L1**, **L2** and **L3** used, similar selectivities were obtained after a reaction time of 20 h with approximatively a ratio 50/50 in EB/EC (Table 2; entries 2, 5 and 8) and 100% EC selectivity in 40 h (Table 2, entries 3, 6 and 9) with 100% styrene conversion. In contrast, the influence of the alkyl chain length ($n = 4$, 3 or 2 carbon atoms between the two phosphorus atoms for **L1**, **L2**, **L3**, respectively) was significantly observed after 1 h. In these later conditions, the best catalytic results were obtained for the longer alkyl chain (**L1**) and the reactivity decreases in the following order: **L1** > **L2** > **L3** (Table 2, entries 1, 4 and 7). As all the Ru(0)NPs display similar mean sizes, the observed differences in their catalytic properties can be correlated to the difference in the flexibility of the alkylchain. A higher flexibility is expected when the number of carbon atoms increases which could induce an easier diffusion of the substrate towards the metal surface. As a consequence of the flexibility of the ligands, a dynamic coordination mode of the alkyl sulfonated diphosphine at the surface of the particle in aqueous solution could be also considered. Mono- or bi-dentate coordination or a mixture of the two modes could take place on Ru(0)NPs. When a monodentate coordination mode is plausible, particularly with the more flexible **L1** protective agent, the steric hindrance decreases on the surface of the particles and therefore access of

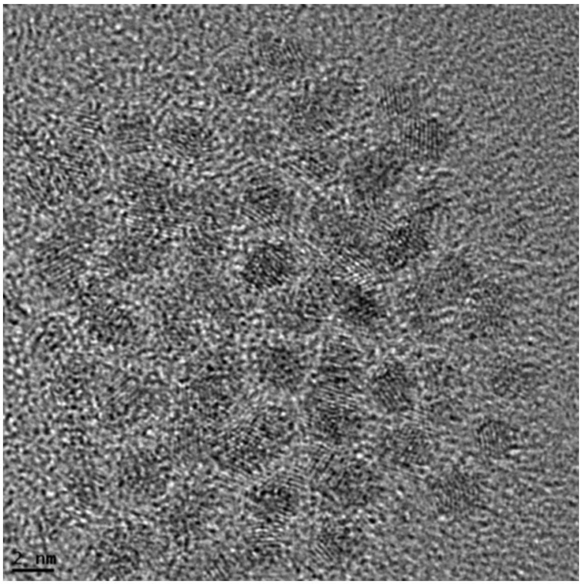

Fig. 3. HRTEM micrograph of Ru(0)NPs stabilized with **L1** ([**L1**]/[Ru] = 0.1).

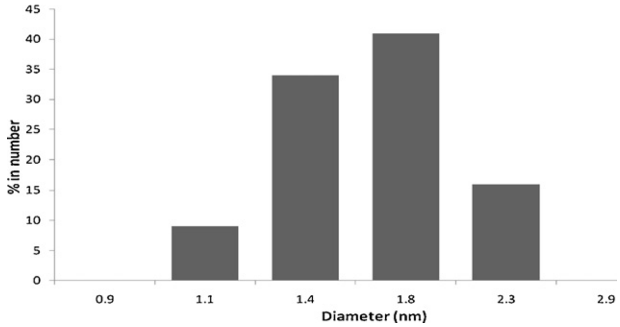

Fig. 4. DLS analysis of Ru(0)NPs stabilized with **L1** ([**L1**]/[Ru] = 0.1).

the substrate increases providing a better reactivity and a more efficient hydrogenation at the beginning of the reaction. Finally, the more lipophilic character induced by a longer alkyl chain could also increase the contact with the substrate and therefore favor the catalysis.

The best Ru/**L1** nanocatalyst was also investigated at 50 °C to evaluate the influence of the temperature on the catalytic performances (Table 2, entries 10–12). The ratio ST/EB significantly increases from 25/75 to 10/90 in 1 h according to the increase of the temperature from 20 °C to 50 °C and the ethylcyclohexane formation (18%) is already observed after a reaction time of 2 h. Finally, the styrene was completely converted in ethylcyclohexane (EC) in 3 h (Table 2, entry 12) in comparison with 40 h at room temperature (Table 2, entry 3). These experiments display the significant influence of the temperature on the catalytic performances in terms of conversion and selectivity which could be attributed to the increase in flexibility of the ligand at the surface of the particles at higher temperature.

3.2.2. Styrene hydrogenation under 10 bar hydrogen pressure and preliminary recycling tests

In a second set of experiments, the influence of the hydrogen pressure on the conversion and the selectivity in ethylbenzene (EB) vs. ethylcyclohexane (EC) ratios was studied according to the choice of the sulfonated diphosphine **L1**, **L2** and **L3** (Table 3) in a molar ratio [**L**]/[Ru] of 0.1. In all cases, a total conversion of the styrene into EB and EC mixture was obtained in 2 h in comparison with 20 h under milder conditions (1 bar H_2 and 20 °C, Table 2). Independently to the choice of the sulfonated diphosphine **L1**, **L2** or **L3**, the hydrogen pressure dramatically impacts the selectivity properties of the catalytic systems. The best performances in terms of selectivity is again achieved with the sulfonated diphosphine **L1**, with 97% of EC in 1 h (Table 3, entry 13) against 90 and 50% for **L2** and **L3** systems (Table 3, entries 17 and 19).

Finally, more drastic reaction conditions such as an increase of temperature to 50 °C (Table 2, entry 12) or of hydrogen pressure up to 10 bar (Table 3, entry 14) similarly modify the behaviour of the catalytic suspensions allowing total reduction of the aromatic ring in respectively 3 and 2 h without visible formation of aggregates. Consequently, the successive hydrogenation of styrene was preliminary carried out with **L1**-stabilized ruthenium nanoparticles (Table 3, entries 15 and 16). No loss of activity was observed

Table 2
Styrene hydrogenation under atmospheric hydrogen pressure catalyzed by alkyl sulfonated diphosphine-stabilized Ru(0)NPs: influence of the ligand.[a]

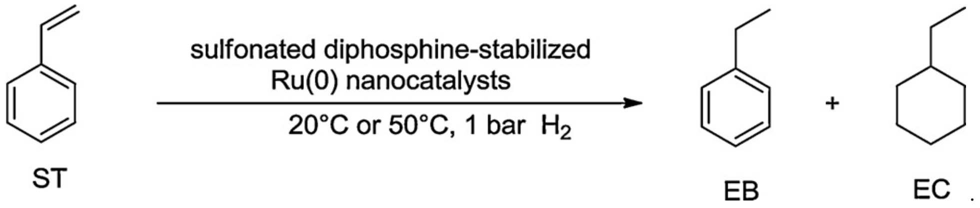

Entry	Sulfonated diphosphine **L**	T (°C)	Time (h)	Products selectivity (%)		
				ST	EB	EC
1	**L1**	20	1	25	75	0
2	**L1**	20	20	0	45	55
3	**L1**	20	40	0	3	97
4	**L2**	20	1	59	40	1
5	**L2**	20	20	0	47	53
6	**L2**	20	40	0	2	98
7	**L3**	20	1	75	24	1
8	**L3**	20	20	0	41	59
9	**L3**	20	40	0	1	99
10	**L1**	50	1	10	90	0
11	**L1**	50	2	0	82	18
12	**L1**	50	3	0	0	100

[a] Reaction conditions: [**L**]/[Ru] = 0.1; ruthenium (3.9×10^{-5} mol), styrene (3.9×10^{-3} mol), 1 bar H_2, water (10 mL).

Table 3
Styrene hydrogenation under 10 bar H_2 catalyzed by sulfonated diphosphine-stabilized Ru(0)NPs: influence of the sulfonated diphosphine ligand (**L**) on the EB/EC ratio.[a]

Entry	Sulfonated diphosphine **L**	Time (h)	Conversion (%)	Products selectivity (%)	
				EB	EC
13	**L1**	1	100	3	97
14	**L1**	2	100	1	99
15[b]	**L1**	2	100	0	100
16[c]	**L1**	2	100	0	100
17	**L2**	1	100	10	90
18	**L2**	2	100	0	100
19	**L3**	1	100	50	50
20	**L3**	2	100	1	99

[a] Reaction conditions: [**L**]/[Ru] = 0.1, ruthenium (3.9×10^{-5} mol), styrene (3.9×10^{-3} mol), RT, water (10 mL)
[b] Recycling of 14.
[c] Recycling of 15.

Table 4
Styrene hydrogenation under atmospheric hydrogen pressure catalyzed by sulfonated diphosphine-stabilized Ru(0)NPs: influence of the [**L3**]/[Ru] ratio on the catalytic activity.[a]

Entry	[**L3**]/[Ru] molar ratio	Time (h)	Conversion (%)	Products selectivity (%)	
				EB	EC
21	0.1	1	25	24	1
22	0.1	20	100	41	59
23	0.2	1	26	26	0
24	0.2	20	100	74	26
25	0.5	1	26	24	2
26	0.5	20	100	84	16

[a] Reaction conditions: Ruthenium (3.9×10^{-5} mol), Styrene (3.9×10^{-3} mol), RT, 1 bar H_2, water (10 mL).

during the second and third runs with the conversion of styrene into 100% ethylcyclohexane in 2 h also, thus justifying the stability and the reusability of the aqueous suspension of the alkyl sulfonated diphosphine-stabilized Ru(0) nanoparticles.

3.2.3. Study of the influence of the [L]/[Ru] metal ratio on styrene hydrogenation at atmospheric hydrogen pressure

To study the influence of the sterical hindrance at the surface of the particles on the catalytic activity of the aqueous colloidal suspension, various [**L3**]/[Ru] ratios (0.1, 0.2 and 0.5) were investigated under atmospheric hydrogen pressure and up to 20 h of reaction time (Table 4). Despite a lower reactivity (Table 2), nanocatalysts prepared with ligand **L3** were chosen for this study as it is the less flexible ligand thus limiting more the substrate diffusion towards the active surface. Whatever the quantity of ligand used for the synthesis of the nanocatalysts, a styrene conversion of ca. 25% in ethylbenzene (EB) is observed after 1 h with only traces of ethylcyclohexane (EC) (Table 4; entries 21, 23, 25). However, all Ru(0) suspensions lead to a total conversion of the substrate in mixtures of ethylbenzene/ethylcyclohexane (Table 4, entries 22, 24, 26) of various ratios in 20 h. Nevertheless, when the [**L3**]/[Ru] ratio increases from 0.1 to 0.5, the proportion of EC significantly decreases from 59 to 16%, respectively (Table 4, entries 22–26). According to the fact that the mean size of the RuNPs does not pertinently change in the presence of more diphosphine ligand (see Table 1, from 1.51 to 1.25 nm with [**L3**]/[Ru] = 0.1 to [**L3**]/[Ru] = 0.2 or 0.5), the difference in selectivity can be explained by a limited access of the aromatic substrate to the nanoparticles surface due to increased sterical hindrance in the presence of more ligand. However, as the ruthenium colloidal suspensions are always stable after 20 h of reaction, we could presume a complete conversion of styrene into ethylcyclohexane for longer reaction times. Thus, a molar ratio of 0.1 seems to be a good compromise between stabilisation and catalytic activity of the particles.

3.2.4. Tetradecene and acetophenone hydrogenation

Finally, preliminary catalytic investigations were performed in the hydrogenation of other unsaturated model substrates containing a C═C or C═O bond for olefin and ketone respectively with the aqueous suspension of the sulfonated diphosphine **L1**-stabilized Ru(0) nanoparticles in a molar ratio [**L1**]/[Ru] of 0.1 (Table 5). First, the tetradecene as an olefinic substrate was studied under 1 bar H_2. In opposition to the previously observed hydrogenation of the exo C═C bond of the styrene (75% after 1 h; entry 1, Table 2), the presence of the long alkyl chain of the tetradecene tends to decrease the olefin hydrogenation as only 7% of conversion are observed in the same reaction time (Table 5, entry 27). This result could be explained by the very low water-solubility of the tetradecene substrate which limits the accessibility of the reducible C═C double bond to the active sites at the surface of the particles which are in water. Moreover, the obtained saturated tetradecane gradually forms an unsoluble phase in which the substrate is more significantly soluble providing a two phase

Table 5
Hydrogenation of tetradecene and acetophenone with **L1**-stabilized Ru(0) NPs.[a]

Entry	Substrate	P (H_2 bar)	Time (h)	Products selectivity (%)
27	Tetradecene	1	1	Tetradecane (7)
28	Tetradecene	1	20	Tetradecane (78)
29	Tetradecene	1	40	Tetradecane (100)
30	Acetophenone	1	2	Phenylethan-1-ol (18)
31	Acetophenone	1	20	Phenylethan-1-ol (84)/cyclohexylethan-1-ol (15)
32	Acetophenone	10	2	Cyclohexylethanol (100)

[a] Reaction conditions: [**L1**]/[Ru] = 0.1, ruthenium (3.9×10^{-5} mol), substrate (3.9×10^{-3} mol), RT, water (10 mL).

mixture, which is not convenient for a conversion increase in the absence of phase transfer agent such as a surfactant [5b,20]. Consequently, a longer reaction time of 40 h was required for a complete conversion (Table 5, entry 29).

The second hydrogenation reaction concerns another interesting substrate, i.e. acetophenone. The interest of this substrate follows from the fact its hydrogenation may lead to several products, mainly due to the competitive hydrogenation of the carbonyl function and the aromatic ring. Thus a 100% conversion is achieved in 20 h with interesting selectivities into phenylethan-1-ol (84%) and cyclohexyl ethan-1-ol (15%) (Table 5, entry 31). Here, we could presume a complete conversion of acetophenone into cyclohexylethan-1-ol for longer reaction times. However, the total conversion into the totally hydrogenated product is also quickly obtained under 10 bar of H_2 (Table 5, entry 32).

4. Conclusions

Our organometallic approach was successfully applied to the synthesis of water-soluble ruthenium nanoparticles with the use of sulfonated diphosphines as stabilizing ligands. The synthesis was carried out in THF in the presence of the alkyl sulfonated diphosphines and the isolated nanoparticles were further easily dispersed in water taking profit of the solubility of the ligands in this solvent. The so-obtained aqueous colloidal solutions are stable for several months, containing ruthenium nanoparticles that display a low size dispersity and very small mean diameters in the range 1.2–1.5 nm depending on the [L]/[Ru] ratio. In addition of controlling their size, the coordination of sulfonated diphosphine ligands on the surface of the Ru(0) particles is of interest for their surface properties and then their water-soluble properties. The aqueous colloidal solutions of these Ru(0) nanoparticles were tested in the hydrogenation of model unsaturated substrates such as styrene, tetradecene and acetophenone in biphasic conditions. The obtained results show that these nanocatalysts are active despite the change of environment they underwent after their dissolution into water. They also show that the reaction selectivity may be tuned in favor of target products as ethylbenzene or phenylethanol-1 as examples depending on the reaction conditions. Finally, preliminary results of recycling are promising for the recovery of these novel water-soluble nanocatalysts.

Acknowledgements

The authors thank L. Datas (LCC-CNRS and UPS-TEMSCAN) for TEM/HRTEM facilities. The authors are grateful to CNRS and the Agence Nationale de la Recherche (ANR-09-BLAN-0194) for the financial support of the SUPRANANO program.

References

[1] (a) G. Schmid, in: K.J Blabunde (Ed.), Nanoscale Materials in Chemistry, Wiley-VCH, New York, 2001;
(b) B. Zhou, S. Han, R. Raja, G. Somorjai, Nanotechnology in Catalysis, Kluwer Academic/Plenum Publisher, New York, 2003;
(c) G. Schmid, Nanoparticles: From Theory to Application, Wiley-VCH, Weinheim, 2004;
(d) H. Ulrich, L. Uzi (Eds.), Nanocatalysis, Series Nanoscience and Technology, Springer, 2007.

[2] D. Astruc, Nanoparticles and Catalysis, Wiley-VCH, Weinheim, 2008.

[3] D. Astruc, F. Lu, J.R. Aranzaes, Angew. Chem., Int. Ed. 44 (2005) 7852.

[4] A. Roucoux, K. Philippot, in: J.G. de Vries, C.J. Elsevier (Eds.), The Handbook of Homogeneous Hydrogenation, Wiley-VCH, 2007.

[5] (a) A. Gual, C. Godard, S. Castillon, C. Claver, Dalton Trans. 39 (2010) 11499;
(b) E. Guyonnet Bile, R. Sassine, A. Denicourt-Nowicki, F. Launay, A. Roucoux, Dalton Trans. 40 (2011) 6524.

[6] (a) Y. Zhu, C.N. Lee, R.A. Kemp, N.S. Hosmane, J.A. Maguire, Chem. Asian J. 3 (2008) 650;
(b) N. Yan, C.X. Xiao, Y. Kou, Coord. Chem. Rev. 254 (2010) 1179;
(c) V. Polshettiwar, R.S. Varma, Green Chem. 112 (2010) 743.

[7] (a) J.K. Whitesell, Chem. Rev. 92 (1992) 953;
(b) R.J. Farrauto, C.G. Bartholomew (Eds.), Fundamentals of Industrial Catalytic Processes, Blackie Academic & Professional, London, 1997.

[8] A. Stanislaus, B.H. Copper, Catal. Rev. Sci. Eng. 36 (1994) 75.

[9] (a) S.-W. Kim, S. Kim, J.B. Tracy, A. Jasanoff, M.G. Bawendi, J. Am. Chem. Soc. 127 (2005) 4556;
(b) O.J. Cayre, N. Chagneux, S. Biggs, Soft Matter 7 (2011) 2211.

[10] (a) B. Cornils, J. Mol. Catal. A: Chem. 143 (1999) 1;
(b) W.A. Herrmann, C.W. Kohlpaintner, Angew. Chem., Int. Ed. Engl. 32 (1993) 524.

[11] (a) C. Larpent, R. Dabard, H. Patin, Inorg. Chem. 26 (1987) 2922;
(b) C. Larpent, R. Dabard, H. Patin, New J. Chem. 12 (1988) 907;
(c) J.P. Genet, M. Savignac, J. Organomet. Chem. 576 (1999) 305.

[12] (a) E.G. Kuntz Fr., Rhône-Poulenc Recherches, Pat. 2.314.910, 1975;
(b) E.G. Guntz, Chemtech 17 (1987) 570.

[13] C. Dupuis, K. Adiey, L. Charruault, V. Michelet, M. Savignac, J.P. Genet, Tetrahedron Lett. 42 (2001) 6523.

[14] (a) E. Ramirez, S. Jansat, K. Philippot, P. Lecante, M. Gómez, A. Masdeu-Bultó, B. Chaudret, J. Organomet. Chem. 689 (2004) 4601;
(b) J. García-Antón, M. Rosa Axet, S. Jansat, K. Philippot, B. Chaudret, T. Pery, G. Buntkowsky, H.-H. Limbach, Angew. Chem. Int. Ed. 47 (2008) 2074.

[15] P.-J. Debouttière, V. Martinez, K. Philippot, B. Chaudret, Dalton Trans. (2009) 10172.

[16] (a) J. Zhong, J. Qu, F. Ye, C. Wang, L. Meng, Y. Yang, J. Colloid Interface Sci. 361 (2011) 59;
(b) Y. Pan, S. Neuss, A. Leifert, M. Fischler, F. Wen, U. Simon, G. Schmid, W. Brandau, W.J. Dechent, Small 11 (2007) 1941.

[17] S. Tilloy, G. Crowyn, E. Monflier, P.W.N.M. van Leeuwen, J.N.H. Reek, New J. Chem. 30 (2006) 377.

[18] C. Pan, K. Pelzer, K. Philippot, B. Chaudret, F. Dassenoy, P. Lecante, M.-J. Casanove, J. Am. Chem. Soc. 123 (2001) 7584 (see also Ref. [14][14(b)]).

[19] (a) B.J. Berne, R. Pecora, Dynamic Light Scattering, Wiley, New York, 1976;
(b) W. Brown, Dynamic Light Scattering: The Method and Some Applications, Clarendon Press Oxford University Press, Oxford [England] New York, 1993.

[20] (a) A. Nowicki, V. Le Boulaire, A. Roucoux, Adv. Synth. Catal. 349 (2007) 2326;
(b) A. Denicourt-Nowicki, A. Ponchel, E. Monflier, A. Roucoux, Dalton Trans. (2007) 5714;
(c) C. Hubert, A. Denicourt-Nowicki, A. Roucoux, D. Landy, B. Leger, G. Crowyn, E. Monflier, Chem. Commun. (2009) 1228.